THE JOURNAL OF BIOLOGICAL CHEMISTRY VOL. 287, NO. 21, pp. 17503–17516, May 18, 2012
© 2012 by The American Society for Biochemistry and Molecular Biology, Inc. Published in the U.S.A.

Slit2 Regulates the Dispersal of Oligodendrocyte Precursor Cells via Fyn/RhoA Signaling*

Received for publication, October 26, 2011, and in revised form, March 15, 2012 Published, JBC Papers in Press, March 20, 2012, DOI 10.1074/jbc.M111.317610

Xiujie Liu[1], **Yan Lu**[1], **Yong Zhang, Yuanyuan Li, Jiazhen Zhou, Yimin Yuan, Xiaofei Gao, Zhida Su, and Cheng He**[2]

From the Institute of Neuroscience and MOE Key Laboratory of Molecular Neurobiology, Neuroscience Research Centre of Changzheng Hospital, Second Military Medical University, Shanghai 200433, China

Background: Secreted by nervous system midline cells Slits regulate neurodevelopmental processes through binding to roundabout receptors (Robos).
Results: Slit2 causes dispersal of oligodendrocyte precursor cells (OPCs) by inducing the association between Robo1 and Fyn.
Conclusion: Robo1 interacts with Fyn to repel the migration of OPCs through RhoA activation.
Significance: Learning how Slit/Robo signaling regulates OPC dispersal is crucial for understanding the distribution of OPCs during central nervous system development.

Oligodendrocyte precursor cells (OPCs) are a unique type of glia that are responsible for the myelination of the central nervous system. OPC migration is important for myelin formation during central nervous system development and repair. However, the precise extracellular and intracellular mechanisms that regulate OPC migration remain elusive. Slits were reported to regulate neurodevelopmental processes such as migration, adhesion, axon guidance, and elongation through binding to roundabout receptors (Robos). However, the potential roles of Slits/Robos in oligodendrocytes remain unknown. In this study, Slit2 was found to be involved in regulating the dispersal of OPCs through the association between Robo1 and Fyn. Initially, we examined the expression of Robos in OPCs both *in vitro* and *in vivo*. Subsequently, the Boyden chamber assay showed that Slit2 could inhibit OPC migration. RoboN, a specific inhibitor of Robos, could significantly attenuate this effect. The effects were confirmed through the explant migration assay. Furthermore, treating OPCs with Slit2 protein deactivated Fyn and increased the level of activated RhoA-GTP. Finally, Fyn was found to form complexes with Robo1, but this association was decreased after Slit2 stimulation. Thus, we demonstrate for the first time that Slit2 regulates the dispersal of oligodendrocyte precursor cells through Fyn and RhoA signaling.

Myelination in vertebrates has evolved to insulate axons and facilitate saltatory conduction of action potentials. Within the CNS, oligodendrocytes are responsible for the formation of the myelin sheath. Oligodendrocytes are derived from oligodendrocyte precursor cells (OPCs),[3] which are originally generated in the ventricular zones of the vertebrate CNS. Before differentiating into myelinating oligodendrocytes, OPCs proliferate, migrate, and then spread throughout the CNS (1, 2). Subsequently, oligodendrocytes undergo morphological maturation, producing myelin components and wrapping axons (3). In the developing mouse CNS, OPCs emerge from the ventral ventricular zone at embryonic day 12.5 (E12.5). Then OPCs generate appropriate numbers of oligodendrocytes through proliferation, spreading widely throughout the CNS around E16 (2, 4, 5). In the rat CNS, OPCs are expressed in a restricted region of the ventricular and subventricular zones at E13. At E16, OPCs spread throughout the gray and white matter in the spinal cord (6). However, the mechanism controlling the migration of OPCs from their site of emergence toward their final destination is poorly understood.

Slit was first identified in *Drosophila* as a molecule secreted by midline cells and was later shown to repel the extension of axons expressing roundabout (Robos) receptors (7–11). Slits can regulate the migration of various cells such as neuronal precursors, glia, and others (12, 13). It has been reported that Slit1–3 are expressed by the floor plate at E11–13 in the rat. Slit2 is highly expressed in the motor neuron regions (10), which are the main original field of the first OPC group around E12.5 (4, 5). The corresponding receptors, Robo1 and Robo2, are also expressed in the motor column at the same time (10, 14). Slit2 remains at its highest expression level in the rat ventral spinal cord but is lower in the dorsal regions (14) when the OPCs begin to spread widely throughout the CNS at E17 (6). Spatial and temporal evidence both hint that Slits may participate in the regulation of OPC migration.

In the present study, we tested the effect of Slit2 on the migration of cultured OPCs. OPCs were shown to express Robo receptors both *in vitro* and *in vivo*. The Boyden chamber assay and the explant migration assay further demonstrated that Slit2 could repel OPC migration. Moreover, Fyn/RhoA signaling was found to mediate the effect of Slit2 on OPC migration. This suggests a previously unknown function of Slit2 on OPC dispersal during development.

* This work was supported by National Key Basic Research Program Grant 2011CB504401 and National Natural Science Foundation Grants 30970999, 31130024, and 31070922.
[1] Both authors contributed equally to this work.
[2] To whom correspondence should be addressed. Fax: 86-21-65492132; E-mail: chenghe@smmu.edu.cn.
[3] The abbreviations used are: OPCs, oligodendrocyte precursor cells; RhoA, Ras homolog gene family, member A; Robos, roundabout receptors; E, embryonic; P, postnatal; PLL, poly-L-lysine; P/D, proximal/distal; SVZ, subventricular zone; NB + B27, neurobasal medium supplemented with 2% B27; CDM, conditioned medium; PFA, paraformaldehyde; ICD, intracellular domain; MBP, myelin basic protein.

EXPERIMENTAL PROCEDURES

Animals and Reagents—All of the animals in this study were obtained from Joint Ventures Sipper BK Experimental Animal (Shanghai, China). The animal experiments were undertaken in accordance with the National Institutes of Health Guide for the Care and Use of Laboratory Animals and with the approval of the Second Military Medical University Committee on Animal Care. All of the inhibitors (Ly294002, PD98059, and Y-27632) were purchased from Calbiochem (Darmstadt, Germany). The antibodies against NG2, MBP, GFAP, and Tuj1 were purchased from Millipore (Billerica, MA), and anti-O4 was from Sigma. The goat antibodies against Robo1 and -2 were from R&D. The anti-Robo1 rabbit antibody used in the immunohistochemistry was from Rockland. The antibodies against *p*-Fyn (Y530) (BS5072) and *p*-Src (Y418) (BS4176), which recognize Tyr^{531} and Tyr^{420} of rat Fyn (NP_036887.1), respectively, were from Bioworld. The anti-Fyn antibody was from Santa Cruz Biotechnology. The rat antibody against PDGFRα was purchased from BD Biosciences. The antibody against RhoA was from Cell Signaling. The antibody for GAPDH was from Kangchen (Shanghai, China). The mouse monoclonal anti-BrdU antibody was from Thermo, and the Olig2 antibody was from Abcam. The TMR Red In-Situ Cell Death Detection Kit was purchased from Roche Applied Science.

Primary Cell Culture—OPCs were isolated from postnatal day 1 (P1) Sprague-Dawley rats as previously described (15, 16). Briefly, the forebrains were removed, diced into fragments in Hanks' buffered salt solution (HBSS), and incubated at 37 °C for 30 min with 0.125% trypsin. The dissociated cells were plated on poly-L-lysine (PLL)-coated tissue culture flasks and grown at 37 °C for 7–10 days in DMEM with 10% fetal calf serum (Invitrogen). The OPCs were collected by shaking the flask overnight at 280 rpm at 37 °C, resulting in 90% purity. The OPCs were then cultured in neurobasal medium supplemented with 2% B27 (NB + B27). To induce the differentiation of precursor cells, OPCs were plated in NB + B27 supplemented with conditioned medium (CDM) from B104 cells for 2–5 days and allowed to proliferate to more than 20,000 cells per cm^2. Then the media were changed to the differentiation medium, which contained 30 nM triiodothyronine. The OPCs were allowed to differentiate for 1–5 days and were identified using O4 or MBP as markers.

Preparation of Conditioned Culture Medium and Purification of Slit2 Protein—The stable cell lines expressing Slit2-myc and RoboN were kindly provided by Professor Xiaobing Yuan and cultured as previously described (17). The cultures were rinsed with Hanks' buffered salt solution and cultured in NB + B27. Two days later, the CDM was collected and filtered with 0.22-μm filters to remove cell debris. The CDM was used in a migration assay after dilution with the appropriate fresh medium at different concentrations. To purify Slit2 protein, stable HEK293 cell lines expressing Slit2-myc were cultured. The protein was purified from the conditioned medium by affinity chromatography using Sepharose conjugated with a Myc antibody (Covance). The purified protein was electrophoresed on a SDS-PAGE gel. The protein concentration was determined by the Bradford method, using BSA as the standard. The same procedure was carried out with the conditioned medium from control HEK293 cells, whose products were used as the control.

Boyden Chamber Migration Assay—The OPC migration studies were performed using a 24-well Boyden chamber (Costar) containing polycarbonate membranes (8 μm pore size), with a slight modification of a previously described protocol (18–20). In brief, the undersides of polyethylene terephthalate filter membranes were coated with PLL or laminin for 2 h at 37 °C. Purified OPCs were seeded into the upper chamber at a density of 1×10^4 cells in 250 μl of culture medium per well. The upper chambers were inserted into the tissue culture wells, and 750 μl of the medium containing the CDM or drugs was added to the lower chambers. After incubation for 16 h at 37 °C, the nonmigratory cells on the upper membrane surface were removed with a cotton swab, and the cells migrating through the membrane pores and invading the underside of the membrane were fixed with 4% paraformaldehyde (PFA) and stained with Coomassie Brilliant Blue. For quantitative assessment, the number of stained, migrating cells presented in five random $\times$20 objective fields per filter were counted under a microscope. At least three independent experiments were performed.

Dissection of Explants and Coculture Experiments—Subventricular zone (SVZ) explants were isolated from postnatal day 5 to 10 (P5-P10) Sprague-Dawley rats as described previously (21). Briefly, aggregates of cells were prepared from stable cell lines expressing Slit2. Each aggregate was placed in the center of a 35-mm dish (Costar) and incubated at 37 °C for 15 min. Sagittal sections of tissue within the borders of the SVZ were dissected out to make SVZ explants of 200–400 μm with a vibratome. Four SVZ explants were isolated and trimmed into blocks of 100–200 μm. Each trimmed explant was embedded in Matrigel and placed near an aggregate. The SVZ explants and aggregates were cultured in NB + B27 and allowed to migrate for 3 days. Then the explants were fixed with 4% PFA and immunostained with an anti-NG2 antibody. The cell nuclei were labeled with Hoechst 33342. The explants located 1 mm or closer to aggregates were imaged with a Nikon fluorescent microscope and analyzed using Image-Pro Plus 5.1 software (Media Cybernetic, Silver Spring, MD). The maximum migration distance from the leading OPCs to the edge of the explants was determined, as was the number of migrated cells. The proximal/distal (P/D) ratio of maximum migration distance was calculated by dividing the maximum migration distance of cells in the proximal quadrant by the maximum migration distance of the cells in the distal quadrant. The P/D ratio of migrated cells was calculated by dividing the number of migrated cells in the proximal quadrant by the number of cells in the distal quadrant, as previously described (21).

Immunohistochemistry and Immunocytochemistry—The cultured cells were gently rinsed with PBS (10 mM sodium phosphate, pH 7.4, and 150 mM NaCl) and then fixed with 4% PFA for 20 min at room temperature. The fixed cells were incubated with primary antibodies overnight at 4 °C and stained with the corresponding secondary antibodies. Immunohistochemistry was performed as described previously (22). Briefly, the animals were anesthetized and intracardially perfused with 4% PFA in 0.1 M phosphate buffer, pH 7.2. The tissues were

removed, post-fixed overnight in the same solution at 4 °C, and then cryopreserved in 20% sucrose in 0.1 M phosphate buffer. Twenty-μm thick frozen sections were cut and incubated in blocking buffer containing 5% BSA and 0.4% Triton X-100 for 30 min and then incubated with the primary antibodies that were diluted in the same blocking buffer overnight at room temperature. After rinsing in PBS, the sections were incubated with the appropriate secondary antibodies conjugated to fluorescein or rhodamine (Jackson ImmunoResearch and Vector Laboratories). Hoechst 33258 (10 μg/ml; Sigma) was used as a nuclear marker. Images were captured using a Nikon fluorescent microscope or a Leica SP2 confocal microscope.

BrdU Incorporation and TUNEL Assays—The proliferation assay was performed as previously described (23). Briefly, the OPCs were purified and plated into PLL-coated 24-well culture dishes (Costar). The media were changed to control CDM or Slit2 CDM after 24 h of culture, at which point BrdU (10 μM, Sigma) was added. After culturing for 16 h, the preparations were fixed in 4% PFA at 4 °C. The PFA was removed 20 min later, and the cells were washed three times with PBS. The preparations were then treated with 2 N HCl for 15 min, 0.1 M sodium borate, pH 8.5, for 15 min, and 0.2% Triton X-100 for 10 min at room temperature. The preparations were washed three times with PBS after each step. The preparations were then successively subjected to an immunocytochemical protocol. The cell nuclei were labeled with Hoechst 33342. The percentage of BrdU-labeled cells *versus* Hoechst-labeled cells was calculated. A TUNEL assay was carried out using the *in situ* cell death detection kit (Roche Applied Science) according to the manufacturer's instructions. In brief, the specimens were fixed in 4% PFA and then processed for antigen retrieval with 0.1 M sodium citrate solution at 90 °C. The specimens were subsequently incubated with the TUNEL reaction solution mixture containing terminal deoxynucleotidyltransferase in a humidified 37 °C chamber for 1 h.

RT-PCR—Total RNA was isolated from dissected rat brains or cultures using TRIzol reagent (Invitrogen). The cDNA synthesis was performed using the thermoscript RT-PCR system (Invitrogen). The following oligonucleotide primers were used: for rat Robo1, the forward primer was 5′-GAATACAGCATGTCTGTAGA-3′ and the reverse primer was 5′-TGTAGCCGTAA-GTATGTGGT-3′; for rat Robo2, the forward primer was 5′-CAACACTCTGGTAACGTGGA-3′ and the reverse primer was 5′-ATCTCAGCCTTCCGAGGACC-3′; for rat Robo3, the forward primer was 5′-CACCATACGTGGAGGAAAGC-3′ and the reverse primer was 5′-GGGCTGGGGATCTCCCTGCA-3′; and for rat GAPDH, the forward primer was 5′-GCATGGCCTTCCGTGTTCCTA-3′ and the reverse primer was 5′-AGTGTTGGGGGCTGAGTTGG-3′.

Western Blot—The oligodendrocytes were rinsed briefly with ice-cold PBS and lysed for 5 min in SDS gel sample buffer. The cell lysates were denatured by boiling for 5 min and then centrifuged for 10 min at 12,000 × *g* and 4 °C. The proteins were separated on an SDS-PAGE gel and then transferred onto nitrocellulose membranes. The membranes were then blocked with 5% nonfat milk in 1× TBST (20 mM Tris, 150 mM NaCl, 1% Tween 20, pH 7.6) and incubated with primary antibodies overnight at 4 °C. To control for differences in protein loading, the membranes were also incubated with an anti-GAPDH antibody. After incubating with horseradish peroxidase (HRP)-conjugated secondary antibodies (Kangchen, Shanghai, China), the immunoreactive bands were visualized by chemiluminescence reagents (ECL, Pierce).

RhoA Activity Assay—The level of active RhoA was determined with the GST-Rhotekin-binding domain as previously described (24). OPCs were plated into the dishes, and Slit2 protein or the control protein was added into the dishes at different times. The cells were washed with ice-cold PBS and lysed in RIPA buffer (50 mM Tris, pH 7.4, 1% Triton X-100, 0.5% sodium deoxycholate, 0.1% SDS, 150 mM NaCl, and a protease inhibitor mixture). The cell lysates were clarified by centrifugation at 12,000 × *g* at 4 °C for 10 min, and equal volumes of lysates were incubated with the GST-Rhotekin-binding domain (20 μg) bound to beads at 4 °C for 60 min. The beads were then washed four times in buffer B (Tris buffer containing 50 mM Tris, pH 7.2, 1% Triton X-100, 150 mM NaCl, and a protease inhibitor mixture) at 4 °C. The bound RhoA proteins were detected by Western blotting using an antibody against RhoA. The amount of GTP-bound RhoA was normalized to the total amount of RhoA in cell lysates as previously described (24), and the results of three independent experiments were statistically analyzed.

Immunoprecipitation and Immunoblotting—The tissue homogenates and cell lysates were prepared as described previously (22) and clarified by centrifugation at 12,000 × *g* and 4 °C for 10 min. An equal volume (200–500 μl) of supernatant was incubated with 2–5 μg of the corresponding antibodies for 3 h at 4 °C. Protein G-agarose beads (Roche Applied Science) were then added for an overnight rotation at 4 °C. The immunoprecipitated samples were then washed three times with lysis buffer, heated in SDS sample buffer in a 50 °C water bath for 20 min, and subjected to SDS-PAGE, immunoblotting, and visualization with enhanced chemiluminescence. The following antibodies were used: monoclonal mouse anti-GFP (mGFP, 1:1,000, Roche), monoclonal mouse anti-HA (mHA, 1:2,000, Abmart), rabbit anti-HA (rHA, 1:3,000, Abcam), and HRP-conjugated secondary antibody (1:10,000, Kangchen).

Statistical Analysis—All data are presented as the mean ± S.E. from at least three independent experiments. The statistical comparisons were made using analysis of variance or Student's *t* test. Any differences were considered significant at $p < 0.05$.

RESULTS

Robo1 Is Expressed in OPCs both in Vitro and in Vivo—To investigate the role of Slits in OPC development, we detected whether the Slit receptors, Robo1, -2, and -3, were expressed in cultured OPCs. The purity of the OPCs was first determined to be over 90% by NG2 or olig2 staining (Fig. 1*A*). We then examined the mRNA levels of Robo1, -2, and -3 in cultured OPCs by RT-PCR. Cultured neurons, astrocytes, and microglia were also examined. We found that both Robo1 and -2 were present in the OPCs, whereas Robo3 was undetectable (Fig. 1*B*). A Western blot analysis revealed the expected protein expression of Robo1 and -2 (Fig. 1*C*). Furthermore, Robo1 and Robo2 could also be detected by immunocytochemistry in cultured OPCs (Fig. 1*D*).

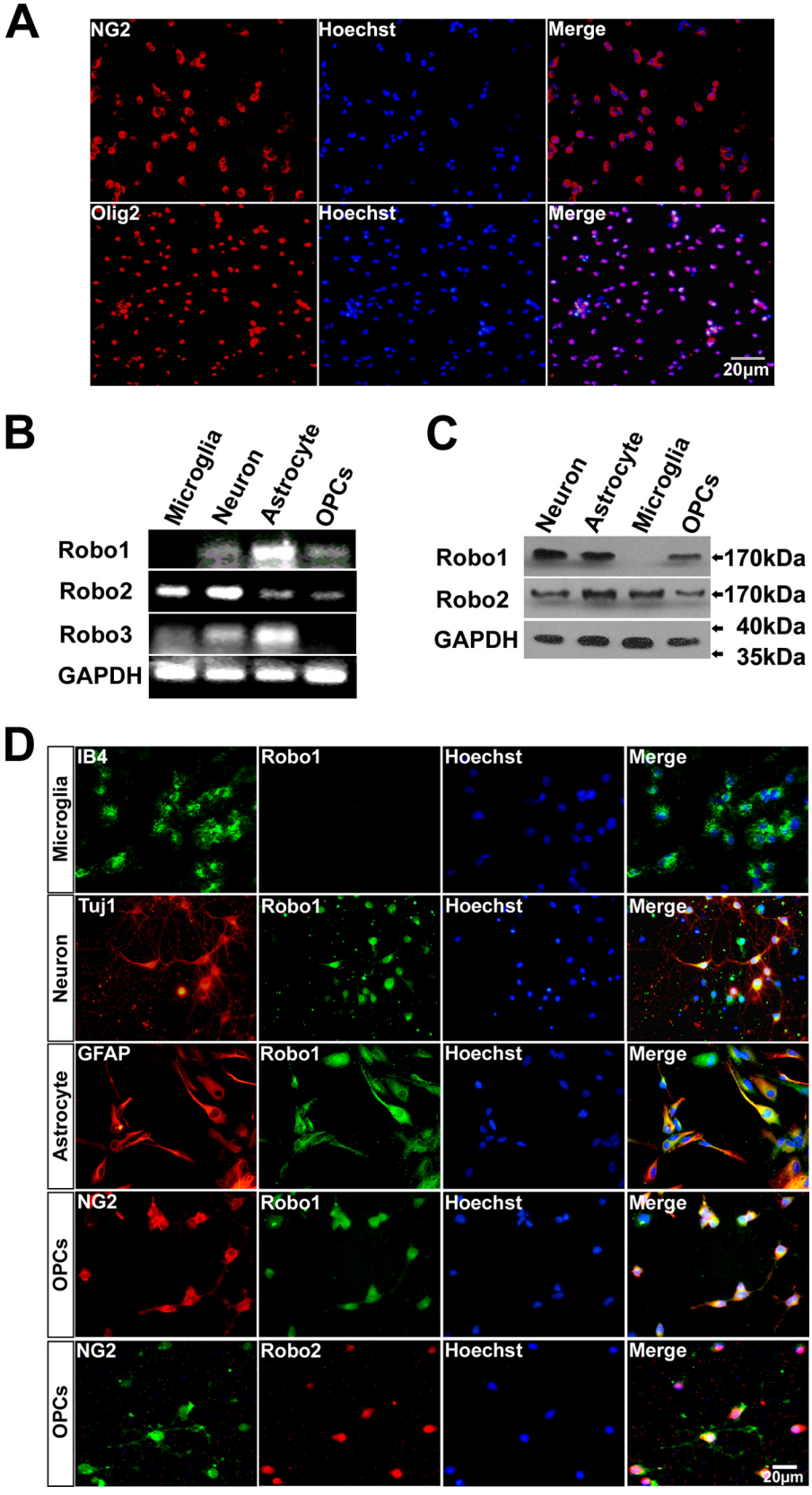

FIGURE 1. **The expression of Robo receptors in OPCs *in vitro*.** *A*, the purified OPCs were identified using NG2 or olig2 as a marker. *B*, the representative RT-PCR results show the mRNA expression of Robo1, -2, and -3 in primary cultures of dissociated cortical neurons, astrocytes, microglia, and OPCs. GAPDH was used as the internal control. *C*, the protein expression of Robo1 and -2 in primary cultures of dissociated cortical neurons, astrocytes, microglia, and OPCs were analyzed by Western blot. GAPDH was used as the internal control. *D*, the expression of Robo1 in primary cultures of dissociated cortical neurons, astrocytes, microglia, and OPCs was determined by immunocytochemical staining using specific markers. The *bottom panel* shows immunostaining of Robo2 in primary cultured OPCs.

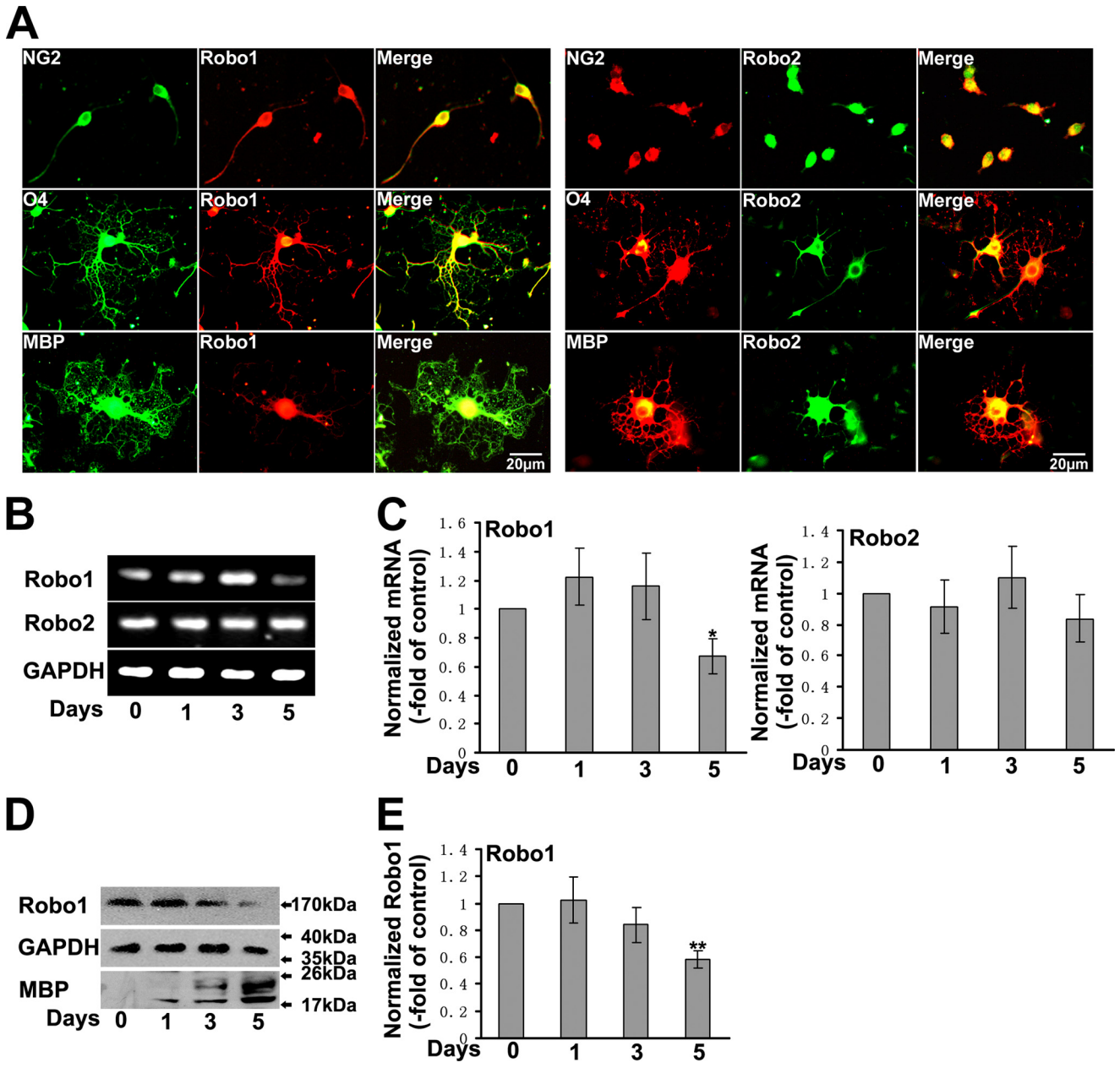

FIGURE 2. **The developmental expression of Robo receptors in cultured OPCs.** *A*, primary cultured OPCs were differentiated for 1, 3, and 5 days and analyzed for Robo1 and -2 expression by immunocytochemical staining. The distribution of Robo1 and -2 and NG2, O4, or MBP is shown by immunofluorescence. *B*, the representative RT-PCR results show the mRNA expression levels of Robo1 and -2 in oligodendrocytes during different developmental stages. GAPDH was used as the control. *C*, the quantification of *B* is presented as -fold of control. Densitometry was used to determine the mRNA levels of Robo1 and -2 in oligodendrocytes during the different developmental stages, and the quantification is presented as -fold of control. *, $p < 0.05$. *D*, the protein expression level of Robo1 in oligodendrocytes at different developmental stages was analyzed with a Western blot. GAPDH was used as control. MBP was used as a marker of oligodendrocyte maturation. *E*, the quantification of *D* is presented as -fold of control. Densitometry was used to determine the level of Robo1 protein in oligodendrocytes at different developmental stages. **, $p < 0.01$.

We next examined the expression patterns of the Robos in developing oligodendrocytes. OPCs were cultured and allowed to differentiate for 1, 3, or 5 days. We found that both Robo1 and -2 were present at all time points during differentiation (Fig. 2*A*). To quantify the levels of Robo1 and -2 mRNA at these points, we performed semiquantitative RT-PCR and found that Robo1 mRNA is slightly down-regulated when the OPCs are differentiated for 5 days (Fig. 2, *B* and *C*). Using MBP as a marker of oligodendrocyte maturation revealed that the protein level of Robo1 decreased with the maturation of oligodendrocytes (Fig. 2, *D* and *E*).

The *in vivo* expression of Robo1 was further confirmed by immunohistochemical staining. First, the antibody against PDGFRα was used to identify OPCs. As shown in Fig. 3*A*, we observed that OPCs were widespread at E16 and the Robo1 receptor was highly co-expressed with the OPCs. This coexpression persisted in the rat spinal cord until adulthood (Fig. 3, *B* and *C*). These results suggested that the Slit receptor Robo1 was expressed in OPCs both *in vitro* and *in vivo*.

Slit2 Repels Cultured OPCs—To investigate the potential roles of Slit2 in OPC migration, OPC motility was investigated using Boyden chamber migration assays. Purified OPCs were

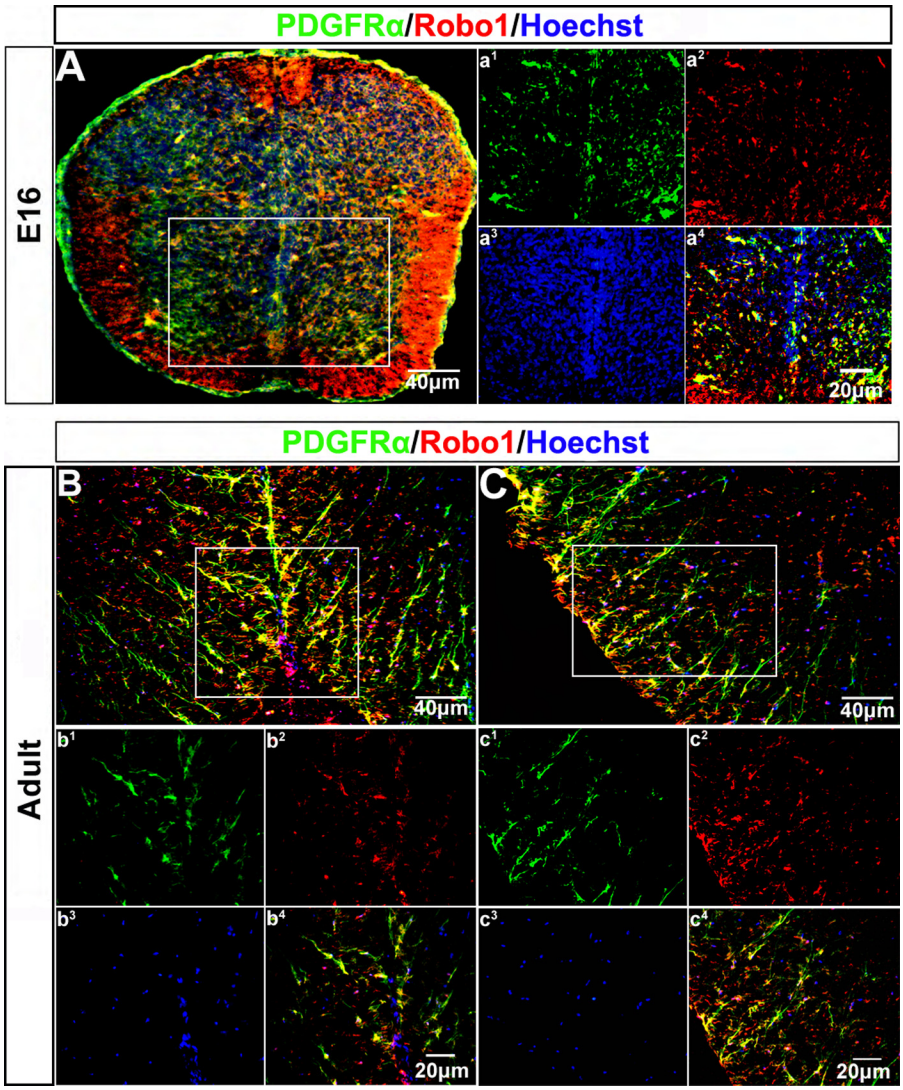

FIGURE 3. **The expression of Robo1 in OPCs *in vivo*.** *A*, immunohistochemical staining for Robo1 and PDGFRα (marker of OPCs) in the E16 mouse spinal cord slices is shown. The tissue slices were immunostained with Robo1 (*red*) and PDGFRα antibodies (*green*). *B* and *C*, immunohistochemical analysis of Robo1 and PDGFRα in adult mouse spinal cord slices. The merged images indicate that Robo1 is expressed in OPCs and widely distributed in the adult mouse spinal cord.

seeded into the upper chamber and allowed to migrate through the filter in response to various concentrations of conditioned media from control HEK293 cells (HEK293 CDM) or HEK293 cells that stably expressed Slit2 (Slit2 CDM) for 16 h. To distinguish the effect of Slit2 CDM from that of HEK293 CDM on OPC migration, we first demonstrated that the OPCs cultured in NB + B27 media with or without different concentrations of HEK293 CDM have similar motility and that no significant changes were found in the HEK293 CDM groups (Fig. 4, *A* and *B*). We next detected the effect of Slit2 on OPC migration. The addition of Slit2 CDM to the lower chamber clearly reduced the number of OPCs that migrated through the filter compared with the control group (Fig. 4, *A* and *C*). As shown in Fig. 4*C*, quantitative analysis revealed that OPC migration through transwell filters was significantly reduced in the groups treated with higher concentrations of Slit2 protein. Interestingly, the addition of Slit2 CDM to the upper chamber along with OPCs caused a significant increase in the number of cells migrating to the lower chamber (Fig. 4*D*). These data suggested that Slit2 acted as a chemorepellent molecule to disperse OPC migration in a concentration-dependent manner. We then confirmed the chemorepellent effect of Slit2 CDM on the OPCs using Slit2 that was purified using Sepharose affinity matrix immobilized with an anti-Myc antibody. The purified Slit2 repelled OPC migration in a dose-dependent manner, with minimal inhibition obtained at 200 ng/ml of Slit2 (Fig. 4*E*). To further examine whether the migration property of OPCs was affected by the coating of filter membrane, we performed Boyden chamber migration assays with laminin-coated transwell filter membranes. As shown in Fig. 4*F*, we found that the repulsive effect of Slit2 on OPCs was not influenced by the laminin coating, as there was no significant difference between the PLL-coated and laminin-coated groups.

Slit2 Does Not Affect Proliferation and Apoptosis of OPCs in Vitro—To evaluate the role of Slit2 in OPC proliferation, we performed a BrdU assay. The OPCs were purified, seeded into PLL-coated dishes, and cultured with BrdU and different concentrations of Slit2 for 16 h. The proliferating cells were labeled with an anti-BrdU antibody and the cell nuclei were labeled with Hoechst. As shown in Fig. 5, *A* and *C*, no difference in the

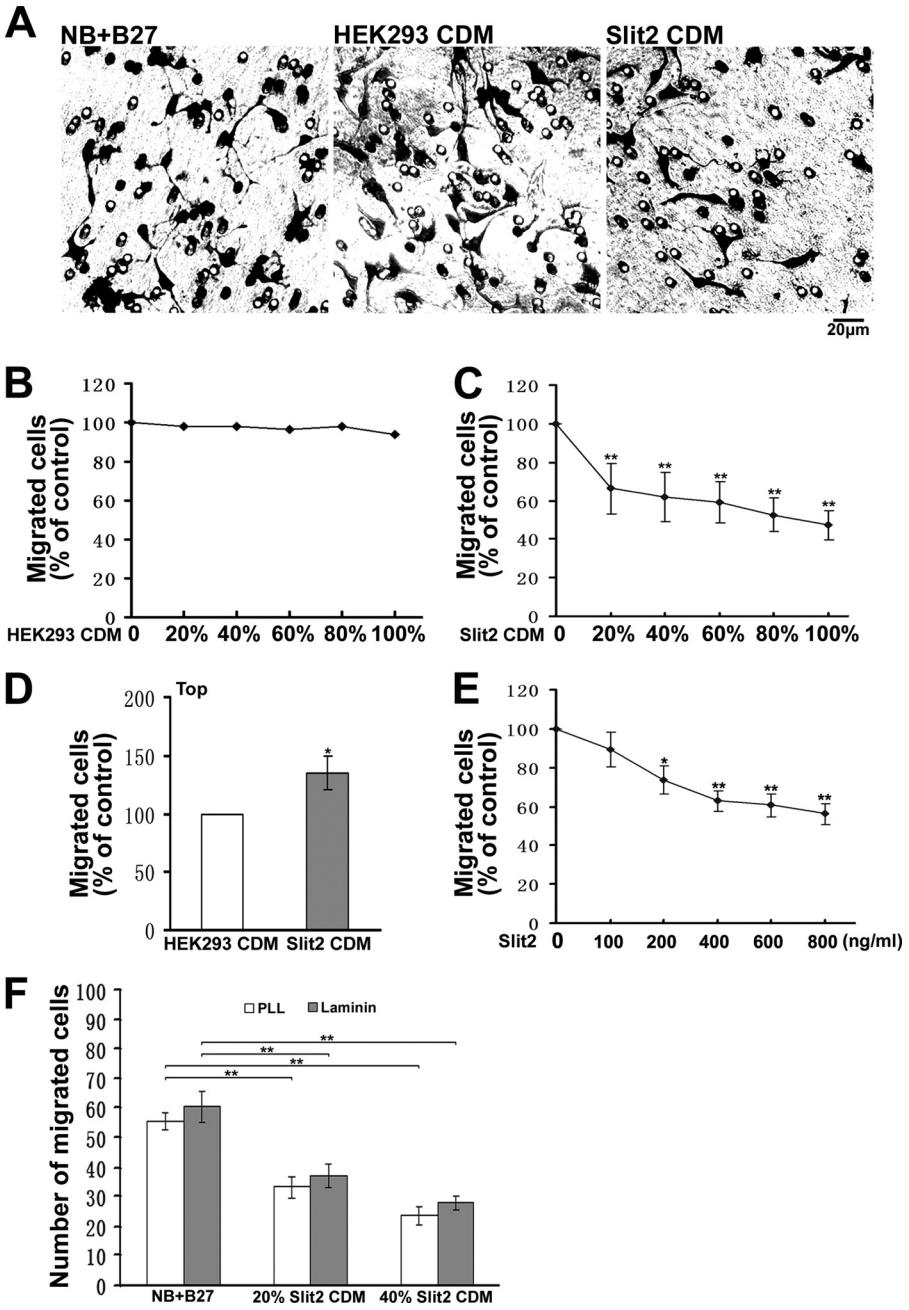

FIGURE 4. **Slit2 repels the migration of OPCs *in vitro*.** *A*, a photomicrograph of cultured OPCs that have transmigrated through transwell membranes. Different concentrations of CDM were added to the bottom compartment. *B* and *C*, the quantitative assessment of cells that migrated through the transwell membranes. The Slit2 CDM significantly reduced cell migration across a range of concentrations (*C*) compared with the HEK293 CDM (*B*). The group incubated without CDM was used as a control. **, $p < 0.01$ *versus* control. *D*, increased migration to the bottom chamber was observed when Slit2 CDM (40%) was added to the top compartment. HEK293 CDM (40%) was used as a control. *, $p < 0.05$ *versus* control. *E*, the dose dependence of the OPC chemorepellent effect of purified Slit2 is shown. The group incubated without Slit2 protein was used as a control. *, $p < 0.05$ and **, $p < 0.01$ *versus* control. *F*, different concentrations of Slit2 CDM were added to the bottom compartment of transwells coated with laminin or PLL. The groups receiving NB + B27 were used as controls. The number of cells migrating under different conditions was quantified. **, $p < 0.01$ *versus* control.

ratio of BrdU positive cells was found between the Slit2 groups and the control group. These data indicated that Slit2 does not influence the proliferation of OPCs in the migration assay. We also performed TUNEL staining to determine the role of apoptosis in the migration assay. As shown in Fig. 5, *B* and *D*, there was no difference in the ratio of TUNEL-positive cells in the Slit2-treated groups and the control group. These results suggested that Slit2 repelled the OPCs without affecting their proliferation and apoptosis.

RoboN Attenuates Effect of Slit2 on OPC Migration—Robo receptors are single transmembrane domain proteins that can bind with Slit2 (7). RoboN, the fragment that contains only the extracellular domain of Robo1, lacks the transmembrane and intracellular domains but retains the capacity to bind with Slit2. Thus, RoboN can be used to competitively inhibit Slit/Robo signaling (12, 25). RoboN was added into the media with Slit2 in the Boyden chamber assay. The addition of RoboN-containing media significantly attenuated the inhibitory effect of Slit2 on

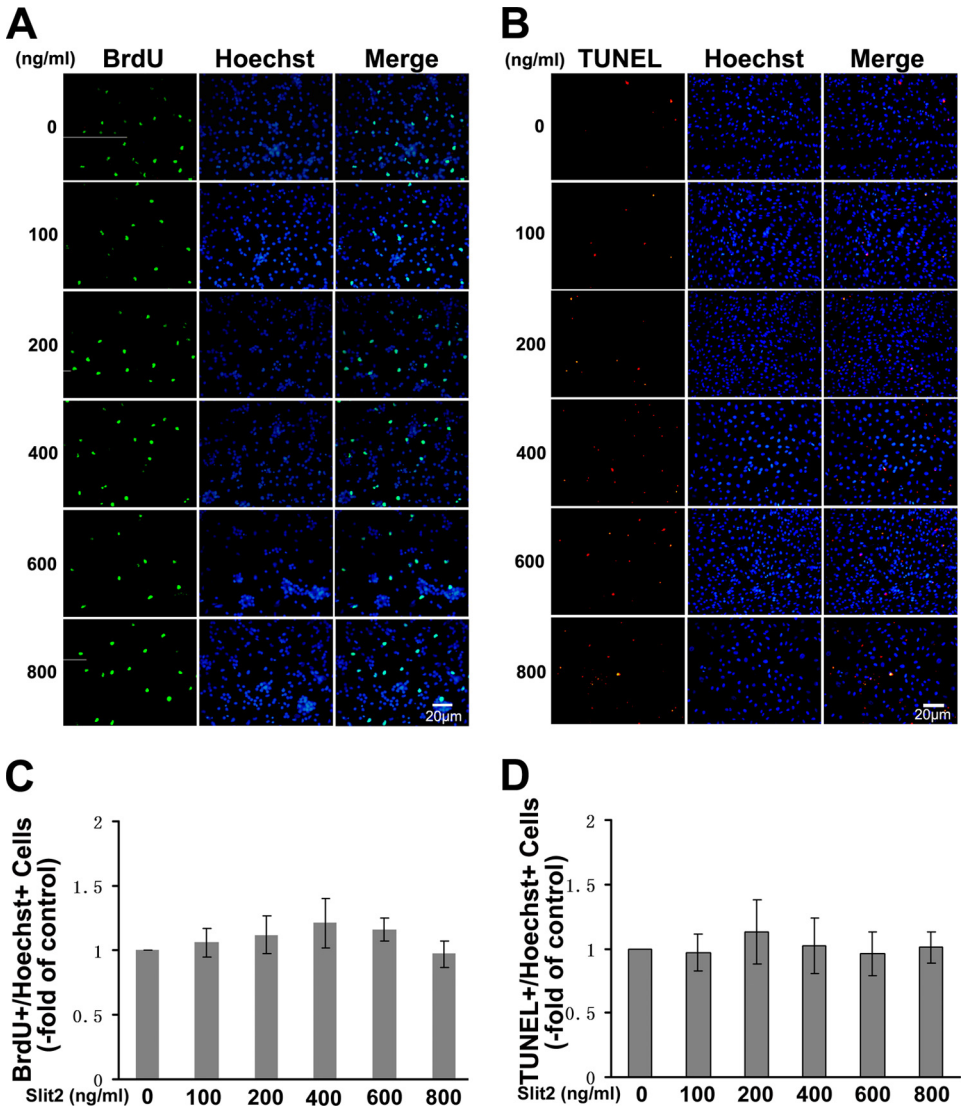

FIGURE 5. **The effect of purified Slit2 on the proliferation and apoptosis of OPCs *in vitro*.** *A*, Slit2 did not affect OPC proliferation. The primary cultured OPCs were seeded in dishes and cultured with BrdU and different concentrations of purified Slit2 protein for 16 h. The proliferating cells were labeled with anti-BrdU (*green*) and the cell nuclei were labeled with Hoechst (*blue*). *B,* Slit2 did not affect OPC apoptosis. The apoptotic cells were detected by TUNEL staining (*red*), whereas the cell nuclei were labeled with Hoechst (*blue*). *C,* the quantification of *A* is presented as -fold of control. The ratio of BrdU-labeled cells was calculated. *D,* the quantification of *B* is presented as -fold of control. The ratio of TUNEL-labeled cells was calculated.

OPCs (Fig. 6, *A* and *B*), indicating that RoboN may act as a dominant-negative binding partner for Slit2 and inhibit Slit2 signaling.

RhoA Is Involved in Slit2-mediated Regulation of OPC Migration—The PI3K/Akt and RhoA pathways have been reported to be involved in mediating cell migration (17, 27). To investigate the downstream mechanism of Slit-Robo signaling, OPCs were treated with pharmacological inhibitors to determine the effect of these inhibitors on Slit2-induced dispersal. As shown in Fig. 7*A*, pretreating OPCs with a Rho kinase-specific inhibitor (Y-27632, 10 μM) (28) greatly attenuated the chemorepellent effect of Slit2 on OPCs. In addition, we observed a slight decline in Slit2-repelled OPC migration after the OPCs were pretreated with LY294002 (10 μM) and PD98059 (20 μM). Neither LY294002 (a specific antagonist of the PI3K/Akt pathway) nor PD98059 (a selective MAPK/Erk inhibitor) significantly rescued the repellent effect of Slit2 on OPCs when compared with that of Slit2 alone. As shown in Fig. 7*B*, dose-response analyses indicated that different concentrations of Y27632 diminished the repellent effect of Slit2 on OPC migration, whereas application of the RhoA inhibitor (Y27632) alone had no effect on OPC migration (Fig. 7*B*). We next tested whether RhoA was activated in the intracellular Slit2 signaling pathway in the OPCs using a GST-fused Rho-binding domain of rhotekin to precipitate GTP-bound RhoA from the cell lysates. As shown in Fig. 7, *C* and *D*, the level of active RhoA increased significantly when the OPCs were stimulated with Slit2. This effect was significant 30–60 min after treatment. Taken together, these results suggested that RhoA may be involved in mediating the repellent effect of Slit2 on OPCs.

Slit2 Down-regulates Fyn Activation in OPCs—It has been reported that Fyn kinase can regulate the activity of the RhoA GTPase (29). Thus, we investigated whether Fyn was involved in Slit2-induced RhoA activity. Rat Fyn kinase is phosphorylated at two tyrosine residues, Tyr^{420} (autophosphorylation site) and Tyr^{531} (negative regulatory site). The autophosphory-

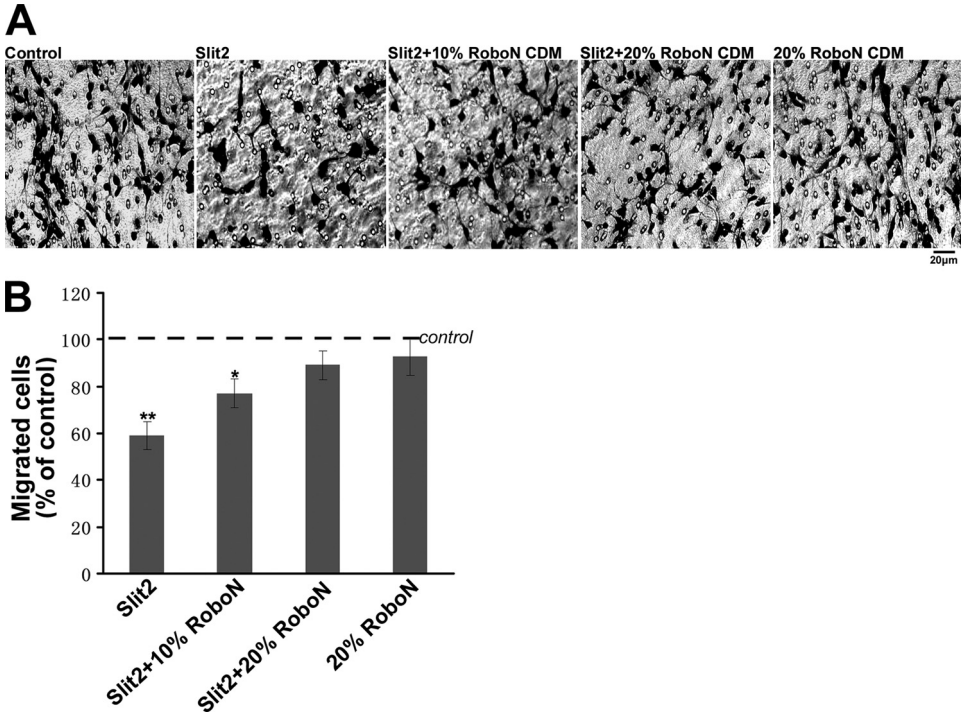

FIGURE 6. **RoboN acts as a specific inhibitor to Slit-Robo signaling.** *A*, a photomicrograph of cultured OPCs that have migrated through transwell membranes is shown. Different concentrations of RoboN CDM with purified Slit2 protein (400 ng/ml) were added to the bottom compartment. *B*, the quantitative assessment of cells migrating through the transwell membranes. RoboN CDM significantly reduced the chemorepellent effect of a range of Slit2 concentrations on the OPCs. The group incubated without CDM was used as a control. The *dotted line* indicates the control level. *, $p < 0.05$ and **, $p < 0.01$ *versus* control.

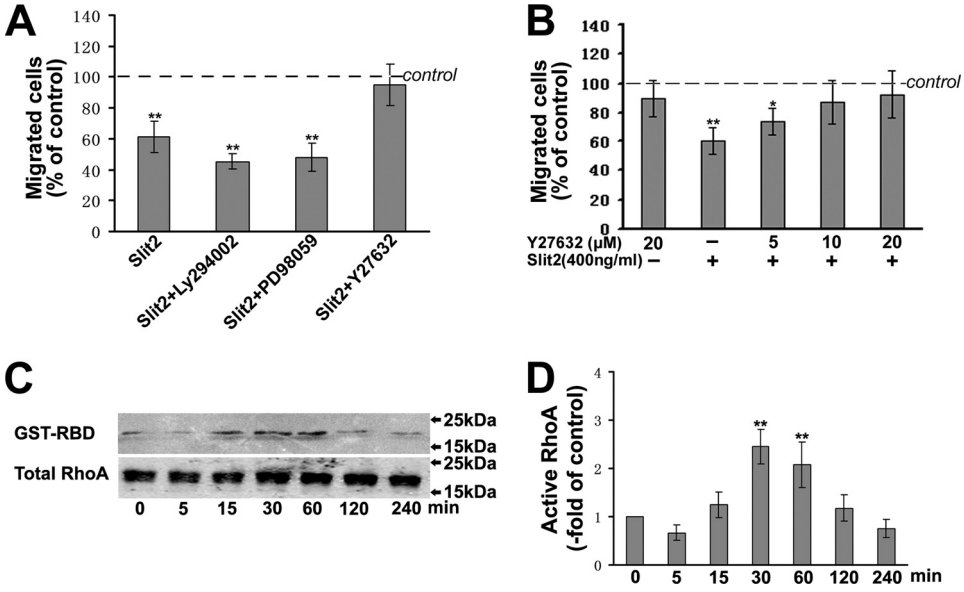

FIGURE 7. **RhoA is required for Slit2 to repel OPC migration.** *A*, OPCs were pretreated with Ly294002 (10 μM), PD98059 (20 μM), and Y-27632 (10 μM) for 30 min. Then the OPCs were plated for Boyden chamber assays and purified Slit2 (400 ng/ml) was added to the bottom compartment. The cells that migrated through the transwell membranes were quantified. The group incubated with NB + B27 medium was used as a control. The *dotted line* indicates the control level. **, $p < 0.01$ *versus* control. *B*, a dose-response analysis revealed the minimal concentration of Y-27632 attenuating the Slit2 (400 ng/ml)-dependent chemorepulsion of the OPCs was 10 μM. The group incubated with NB + B27 medium was used as a control. The *dotted line* indicates the control level. *, $p < 0.05$ and **, $p < 0.01$ *versus* control. *C*, the OPCs were cultured and stimulated with (400 ng/ml) Slit2, using untreated cells as the control. The OPCs were lysed at various time points after stimulation. The RhoA activation in the OPCs was determined by pulldown assays with the Rho-binding domain of rhotekin. *D*, the quantification of *C* is presented as -fold of control. The amount of GTP-bound RhoA was normalized to the amount of total RhoA. **, $p < 0.01$.

lation of Tyr^{420}, which resides within the kinase activation loop, leads to the activation of Fyn, whereas the phosphorylation of C-terminal Tyr^{531} inhibits Fyn kinase activity (30, 31). Thus, we investigated the effects of Slit2 stimulation on Fyn activity in OPCs by detecting Fyn phosphorylation status. The phosphorylation of Fyn Tyr^{531} increased significantly after Slit2 treatment (Fig. 8, *A* and *B*), whereas the phosphorylation of Tyr^{420} decreased significantly (Fig. 8, *A* and *C*). This result indicates Fyn inactivation. Overall, our data provide evidence that Slit2 down-regulated the activation of Fyn in OPCs.

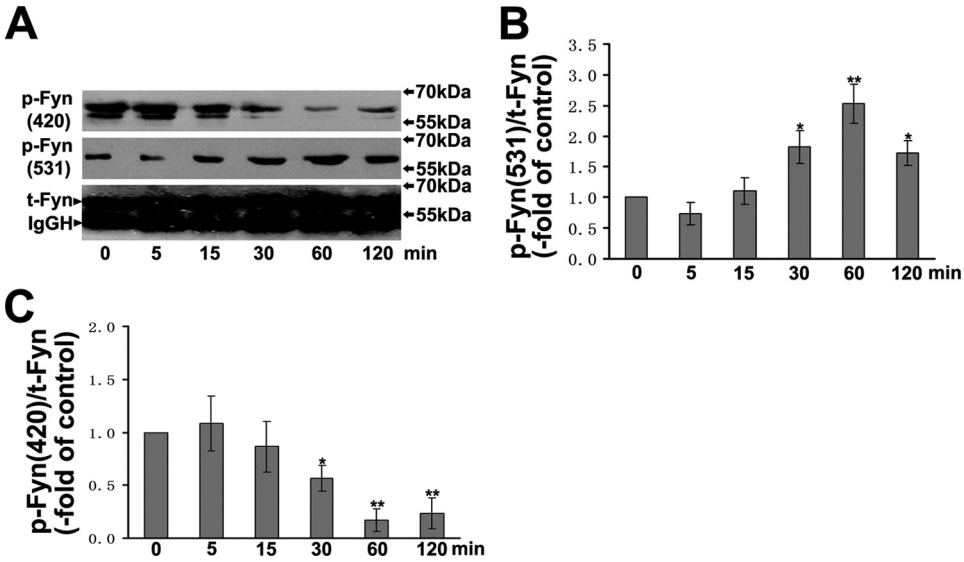

FIGURE 8. **Slit2 regulates the activity of Fyn in rat OPCs.** *A*, OPCs were cultured and stimulated with (400 ng/ml) Slit2, using untreated cells as the control. The cells were then lysed at various time points after stimulation. The phosphorylation of rat Fyn (*p-Fyn*) at Tyr^{420} or Tyr^{531} was analyzed by immunoprecipitation followed by immunoblotting with a *p*-c-Src (Y418) or *p*-Fyn (Y530) antibody. *B* and *C*, the band intensity of Fyn *p*-Tyr^{531} or *p*-Tyr^{420} was normalized to that of total Fyn (*t-Fyn*). The quantification is presented as -fold of control. *, $p < 0.05$; **, $p < 0.01$.

Robo1 Forms Complexes with Fyn—The Robo1 receptor is a transmembrane receptor that mediates cellular responses to slits (7, 9). The Slit2-mediated induction of Fyn phosphorylation in OPCs prompted us to test whether the Robo1 receptor forms a complex with this protein. The GFP-tagged intracellular domain (ICD) of Robo1 and/or HA-tagged full-length Fyn were transfected into HEK293T cells. When an anti-GFP antibody was used to immunoprecipitate the cell lysates from cells co-transfected with GFP-Robo1-ICD and HA-Fyn, HA-Fyn was detected in the precipitates (Fig. 9*A*). Conversely, when the co-transfected cell lysates were subjected to immunoprecipitation with anti-HA, GFP-Robo1-ICD was also detected in the precipitates (Fig. 9*B*). These data suggested that the specific association between GFP-Robo1-ICD and HA-Fyn existed in co-transfected HEK293T cells. To examine whether Robo1 and Fyn form a natural complex in OPCs, OPC lysates were immunoprecipitated with anti-Robo1 and immunoblotted with anti-Fyn. As shown in Fig. 9*C*, Fyn was detected in the anti-Robo1 precipitates but not the IgG precipitates. Thus, endogenous Robo1 and Fyn formed a co-precipitable protein complex in OPCs. We then examined whether Robo1 and Fyn were expressed in OPCs. An immunocytochemical analysis was carried out in OPCs. As shown in Fig. 9*F*, fluorescent imaging showed the expression of Robo1 (red) and Fyn (green) in the OPCs. The merged image revealed that Robo1 and Fyn were expressed in the same OPCs. To investigate whether Slit2 can regulate the endogenous interaction between Fyn and Robo1, conditioned medium containing the Slit2 protein was added to the OPC culture medium for 30 min before the cell lysates were prepared. Slit2 significantly reduced the binding of Fyn to Robo1 (Fig. 9, *D* and *E*), suggesting that extracellular Slit2 regulates the endogenous association between Fyn and Robo1.

Slit2 Repels OPCs from SVZ—The postnatal SVZ surrounding the lateral ventricles contains OPCs, which are recognized as a source of forebrain oligodendrocytes in neonates (32). Therefore, we assessed whether the OPCs in SVZ tissue explants in culture respond to the Slit2 gradient. As shown in Fig. 10*A*, the SVZ tissue explants dissected from P5–P10 rats were plated in the proximity of aggregates of wild-type or Slit2-expressing HEK293T cells in Matrigel for 72 h. After the OPCs were identified by immunostaining with an anti-NG2 antibody, the maximum migration distances and number of migrated cells were examined. As shown in Fig. 10, *B* and *C*, the distribution of migrated cells in the explant co-cultures were mostly symmetrical (with 11 symmetric explants of 12 explants). However, most of the explant co-cultured with aggregates of HEK293T cells expressing Slit2 were asymmetrical (with 13 asymmetric explants of 16 explants). The number of migrated OPCs in the quadrant proximal to the Slit2 cells was significantly lower than that in the distal quadrant. Additionally, the mean maximum migration distance of the OPCs close to Slit2 was significantly shortened. Moreover, the Slit2-induced asymmetric migration was prevented when the media contained Y27632 (with 8 symmetric explants of 10 explants) and RoboN (with 10 symmetric explants of 12 explants). These results indicated that Slit2 acted as a chemorepellent to expel the OPCs from the SVZ.

DISCUSSION

Newborn OPCs migrate away from the ventral midline immediately after being generated and disperse throughout the developing CNS before birth (2, 6). OPC migration requires the timely expression of proteins that contribute to cell motility, neuron-glial adhesion, and cytoskeletal regulation (33, 34). Several cues, such as netrin1 and semaphorin 3A (which are secreted by floor plate cells at an early developmental stage), have been reported to disperse OPCs and facilitate their migration to target regions (18, 19, 35, 36). Slits are also secreted by the floor plate and have been reported to be involved in the motility of various cells. In our study, we found that Slit2 inhibited OPC migration during the transwell and explant tissue assays. Interestingly, OPC migration was inhibited when Slit2

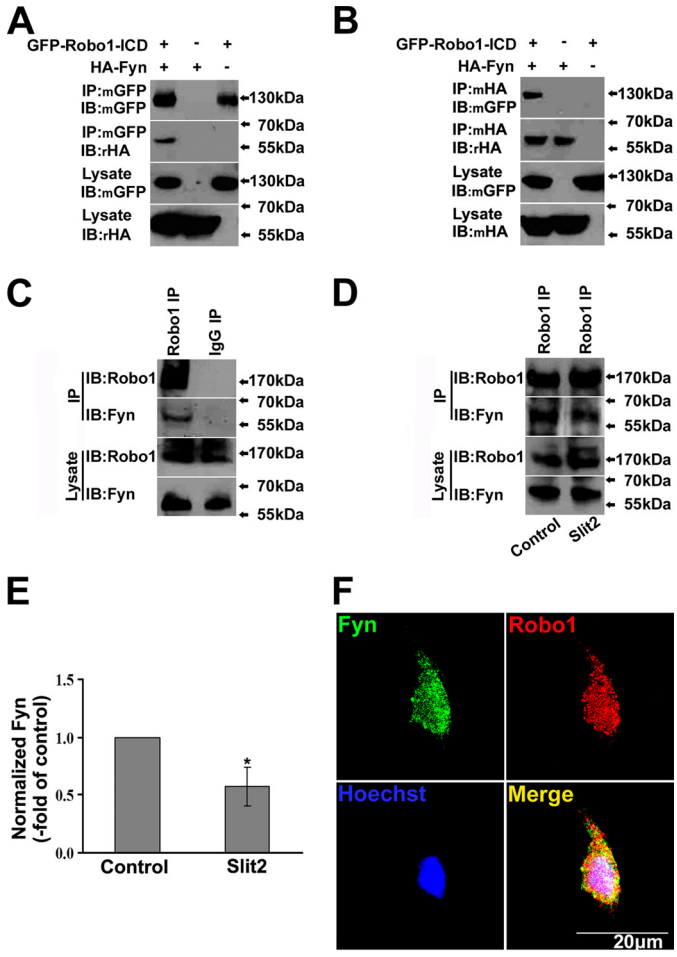

FIGURE 9. **The identification of Fyn as a Robo1-interacting molecule.** *A* and *B*, the binding of Fyn to Robo1 in transfected HEK293T cells. GFP-Robo1-ICD and/or HA-Fyn were expressed in cells. The proteins were immunoprecipitated (*IP*) with GFP or an HA-specific antibody, and the precipitates were subjected to immunoblotting (*IB*) with antibodies against HA or GFP as indicated. *C*, the immunoprecipitation shows that endogenous Robo1 interacts with Fyn in primary cultured OPCs. The goat IgG was used as the immunoprecipitation control. *D*, Slit2 significantly reduced the binding of Fyn to Robo1 after Slit2 stimulation. The OPCs were treated with Slit2 for 30 min. The OPCs treated with conditioned medium from wild-type HEK293T cells were used as the control. *E*, the quantification of *D* is presented as -fold of control. The band intensity of Fyn in the precipitates was normalized to that of Fyn in the lysates. *, $p < 0.05$. *F*, the co-expression of Robo1 and Fyn in primary rat OPC cultures was shown by immunocytochemical staining. *Green*, stained with anti-Fyn; *red*, stained with anti-Robo1.

was added into the bottom chamber in the Boyden chamber migration assay. Conversely, OPC migration was promoted when Slit2 was added to the upper chamber. Thus, Slit2-repelled OPC movement may be asymmetrical, with the cells moving toward the low concentration of Slit2. Similar repulsive effects of the Slit2 gradient were confirmed in explanted SVZ tissues (Fig. 10). One possible interpretation of these results may be that OPCs preferentially migrate down a gradient of Slit2. It has been reported that Slit2 shows a typical gradient distribution, with the highest expression in the ventral midline of the CNS and a gradient running across to the dorsal side (14). In the present study, we found that Robo1 receptors were highly expressed in the migrating OPCs *in vivo* (Fig. 3). With consideration of the high level of temporal and spatial consistency between the distribution pattern of Slit2-Robo1 and OPC spreading routes, we hypothesized that Slit2 may act as a repellent molecule to disperse OPCs and direct them away from their ventral origins.

The proteins in the Rho family of small GTPases have been reported as central players in the regulation of actin cytoskeleton assembly, adhesion formation, neurite outgrowth, axon guidance, and cell migration, during which RhoA signals the formation and maturation of focal adhesions associated with actin stress fiber bundles (37–39). The formation of membrane protrusions is an early step in the process of cell migration. When the ratio of activity of these small GTPases is no longer optimal for the protrusion and polarization of the cell, migration will be influenced (40). Constitutively active RhoA may impede cell motility (20, 41, 42). One of the downstream effectors of RhoA is Rho kinase, which can be effectively inhibited by the compound Y-27632 (28, 43). Inhibiting Rho kinase stimulates membrane protrusion and promotes cell migration (40, 44, 45). Here, we observed that the chemorepellent effect of Slit2 on OPC migration was significantly attenuated when the cells were pretreated with Y-27632. We found that active RhoA significantly increased in the OPCs treated with Slit2, which suggested that the binding of Slit2 to Robos led to the activation of RhoA in the OPCs. There are controversial reports regarding the effects that Slit2 has on RhoA activity. One study showed evidence that Slit2 increased RhoA activity in Robo1-expressing HEK293 cells but did not affect RhoA activity in SVZ cells (46). However, another study demonstrated that Slit2 down-regulated RhoA activity in granule cells in a Ca^{2+}-dependent manner (17). In our study, we found that Slit2 up-regulated RhoA activity in OPCs. This effect was observed at least 30 min after Slit2 stimulation. Our data are similar to the recent report by Kennedy *et al.* (47), who found that RhoA activity was up-regulated early in OPC development and then later decreased in oligodendrocytes. The inhibition of RhoA activity disrupted netrin1-dependent OPC chemorepulsion. Thus, it is likely that the difference in cell type may account for these conflicting reports about the distinct effects of Slit2 on RhoA activity.

Although the regulatory role of Slit2 on the activity of RhoA has been widely reported (17, 46, 48), the mechanism by which Slit2 alters RhoA activity remains elusive. Prasad *et al.* (27) found that Slit2 can block the CXCL12-induced activation of Src and Lck kinases and inhibit the CXCL12-induced chemotaxis and transendothelial migration of T cells. Wong *et al.* (26) reported that PP2 treatment blocked the Slit2-induced growth cone collapse of the chick retinal ganglion cell, suggesting that activation of the Src family kinases is required for Slit2-induced growth cone collapse. It seems that the Src family kinases may be involved in the Slit2-induced signaling pathway. Thus, the roles of Src family members in the development of OPCs need to be further studied. Five members of the Src kinase family are expressed in the mammalian CNS, including Src, Fyn, Yes, Lck, and Lyn (30). Among them, Fyn, Lyn, and Yes are expressed in OPCs. However, only Fyn is both expressed and activated in OPCs (49, 50). Fyn has been reported to regulate the differentiation of oligodendrocytes (29, 49). Additionally, Fyn also plays roles in many cellular processes, including cell adhesion and migration (51). In the present study, we found Slit2 treatment significantly increased the phosphorylation of

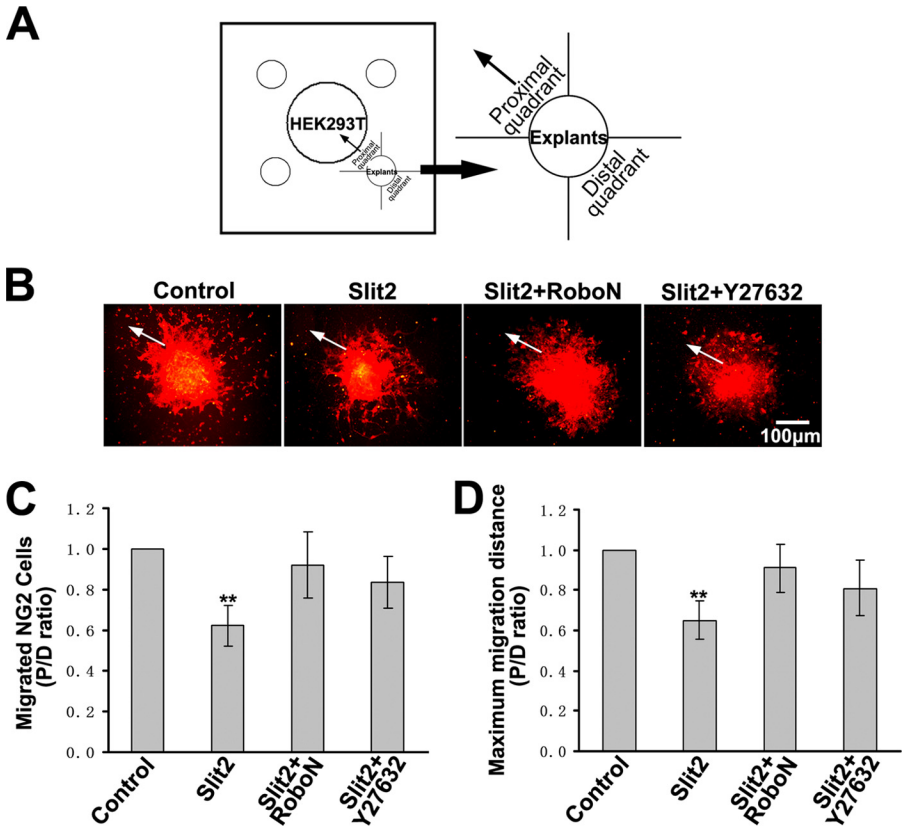

FIGURE 10. **The effect of Slit2 on OPCs migrating from SVZ explants.** *A*, a schematic diagram of the tissue explant migration assay is shown. Four SVZ explants (*open circles*) were cultured on one Matrigel-coated coverslip. Aggregates of wild-type HEK293 cells or cells stably expressing Slit2 were placed at the center of the coverslip. The explants were divided into four parts. *B*, the SVZ explants were co-cultured with aggregates of wild-type HEK293 cells (*Control*) or with aggregates of HEK293 cells stably expressing Slit2 under various conditions for 72 h. The anti-NG2 immunostained images show the asymmetric or symmetric distribution of NG2 cells migrating from the edge of the explants. The *arrows* indicate the direction toward the aggregates. *C*, the P/D ratio of migrated cells was calculated by dividing the number of migrated cells in the proximal quadrant by the number of cells in the distal quadrant. The P/D ratio of NG2 cells migrating out of the explants under various conditions was normalized to a control. **, $p < 0.01$ *versus* control. *D*, the P/D ratio of maximum migration distance was calculated by dividing the mean maximum migration distance of leading cells in the proximal quadrant by those in the distal quadrant. The P/D ratios of the maximum migration distances of NG2 cells under various conditions were normalized to a control. **, $p < 0.01$ *versus* control.

Fyn at the regulatory C-terminal tail residue Tyr^{531} and decreased the autophosphorylation of Tyr^{420}, which resides within the kinase activation loop. These data indicate that Slit2 stimulation may inactivate Fyn in OPCs. Interestingly, this effect was significant 30 min after Slit2 treatment, which was consistent with the time course of RhoA activation. The activity of the RhoA GTPase can be regulated by Fyn kinase. It has been reported that Fyn phosphorylates and activates p190 RhoGAP, which in turn inactivates RhoA in oligodendrocytes (29, 52, 53). In our study, the time course of Fyn inactivation correlated with that of RhoA activation. In combination with the finding that Fyn forms complexes with Robo1, these results support the hypothesis that Slit2 may deactivate Fyn and then activate RhoA through Robo1 signaling in OPCs.

In this study, we have found that Slit2 can regulate the activity of Fyn through the induction of protein phosphorylation. However, Liu *et al.* (54) claimed that no substantial effect on Fyn (tyrosine) phosphorylation was detected after treating cortical neurons with Slit-conditioned medium. This inconsistency may be due to the different detection systems used. Additionally, we determined that the association between Robo1 and Fyn in primary OPCs was reduced by Slit2 treatment. One possibility may be that Slit2 treatment attenuated the binding of Fyn to Robo1 receptor complexes and deactivated Fyn in OPCs. It would be interesting to further explore the detailed mechanisms of Fyn involved in the signaling pathway that modulates the developmental processes of OPCs.

A previous study showed that Slit can increase the interaction between Robo1 and slit-robo Rho GTPase activating protein 1 (srGAP1) and regulate the activities of several Rho GTPases (46). In this study, we found that Slit2 can attenuate the endogenous association between Fyn and Robo1 in primary OPCs. Our results indicate that Robo1 may play a role in regulating cell migration by interacting with various downstream signaling molecules. Several other molecular regulators of OPC migration have been proposed, including netrin1, semaphorins, and ephrin (35, 55, 56). Slit1, -2, and -3 and Netrin1 are coexpressed both in the floor plate and in a number of locations throughout the nervous system (57). It seems likely that the guidance of oligodendrocyte precursors to their appropriate domains will involve multiple guidance cues. Brose *et al.* (10) reported that Slit2 interacts with Netrin1. Additionally, Robo1 was found to bind to the Netrin1 receptor Deleted in Colorectal Cancer and silence netrin1 attraction in the presence of Slit (58). Deleted in Colorectal Cancer was reported to form a complex with Fyn and regulate the activity of RhoA in oligodendrocytes (59). In our study, the Slit2 signaling pathway involved in regulating OPC migration includes Fyn and RhoA and is similar

to that of netrin1. Robo1 was also found to associate with Fyn. This evidence suggests that an extrinsic change in interaction may reflect an intrinsic cross-talk in these signaling pathways. We propose that Robo1, DCC, and Fyn may form complexes and that the molecules in these complexes may be induced by both Slit2 and netrin1.

In conclusion, it was confirmed that Fyn associates with Robo1 and regulates the Slit2-induced activation of RhoA. These results may shed new light on Slit-Robo signaling in cell migration.

Acknowledgment—We thank Professor Xiaobing Yuan (Shanghai Institute of Neuroscience, Chinese Academy of Sciences) for providing the Slit2-myc cell line and cells expressing RoboN.

REFERENCES

1. Zhu, X., Hill, R. A., and Nishiyama, A. (2008) NG2 cells generate oligodendrocytes and gray matter astrocytes in the spinal cord. *Neuron Glia Biol.* **4,** 19–26
2. Kessaris, N., Fogarty, M., Iannarelli, P., Grist, M., Wegner, M., and Richardson, W. D. (2006) Competing waves of oligodendrocytes in the forebrain and postnatal elimination of an embryonic lineage. *Nat. Neurosci.* **9,** 173–179
3. Miller, R. H., and Mi, S. (2007) Dissecting demyelination. *Nat. Neurosci.* **10,** 1351–1354
4. Rowitch, D. H. (2004) Glial specification in the vertebrate neural tube. *Nat. Rev. Neurosci.* **5,** 409–419
5. Richardson, W. D., Kessaris, N., and Pringle, N. (2006) Oligodendrocyte wars. *Nat. Rev. Neurosci.* **7,** 11–18
6. Pringle, N. P., and Richardson, W. D. (1993) A singularity of PDGF α-receptor expression in the dorsoventral axis of the neural tube may define the origin of the oligodendrocyte lineage. *Development* **117,** 525–533
7. Li, H. S., Chen, J. H., Wu, W., Fagaly, T., Zhou, L., Yuan, W., Dupuis, S., Jiang, Z. H., Nash, W., Gick, C., Ornitz, D. M., Wu, J. Y., and Rao, Y. (1999) Vertebrate slit, a secreted ligand for the transmembrane protein roundabout, is a repellent for olfactory bulb axons. *Cell* **96,** 807–818
8. Nguyen Ba-Charvet, K. T., Brose, K., Marillat, V., Kidd, T., Goodman, C. S., Tessier-Lavigne, M., Sotelo, C., and Chédotal, A. (1999) Slit2-mediated chemorepulsion and collapse of developing forebrain axons. *Neuron* **22,** 463–473
9. Kidd, T., Bland, K. S., and Goodman, C. S. (1999) Slit is the midline repellent for the robo receptor in *Drosophila*. *Cell* **96,** 785–794
10. Brose, K., Bland, K. S., Wang, K. H., Arnott, D., Henzel, W., Goodman, C. S., Tessier-Lavigne, M., and Kidd, T. (1999) Slit proteins bind Robo receptors and have an evolutionarily conserved role in repulsive axon guidance. *Cell* **96,** 795–806
11. Challa, A. K., Beattie, C. E., and Seeger, M. A. (2001) Identification and characterization of roundabout orthologs in zebrafish. *Mech. Dev.* **101,** 249–253
12. Wu, W., Wong, K., Chen, J., Jiang, Z., Dupuis, S., Wu, J. Y., and Rao, Y. (1999) Directional guidance of neuronal migration in the olfactory system by the protein Slit. *Nature* **400,** 331–336
13. Xu, Y., Li, W. L., Fu, L., Gu, F., and Ma, Y. J. (2010) Slit2/Robo1 signaling in glioma migration and invasion. *Neurosci. Bull.* **26,** 474–478
14. Wang, K. H., Brose, K., Arnott, D., Kidd, T., Goodman, C. S., Henzel, W., and Tessier-Lavigne, M. (1999) Biochemical purification of a mammalian slit protein as a positive regulator of sensory axon elongation and branching. *Cell* **96,** 771–784
15. Mi, S., Miller, R. H., Lee, X., Scott, M. L., Shulag-Morskaya, S., Shao, Z., Chang, J., Thill, G., Levesque, M., Zhang, M., Hession, C., Sah, D., Trapp, B., He, Z., Jung, V., McCoy, J. M., and Pepinsky, R. B. (2005) LINGO-1 negatively regulates myelination by oligodendrocytes. *Nat. Neurosci.* **8,** 745–751
16. Liu, X., Li, Y., Zhang, Y., Lu, Y., Guo, W., Liu, P., Zhou, J., Xiang, Z., and He, C. (2011) SHP-2 promotes the maturation of oligodendrocyte precursor cells through Akt and ERK1/2 signaling *in vitro*. *PLoS One* **6,** e21058
17. Guan, C. B., Xu, H. T., Jin, M., Yuan, X. B., and Poo, M. M. (2007) Long-range Ca^{2+} signaling from growth cone to soma mediates reversal of neuronal migration induced by slit-2. *Cell* **129,** 385–395
18. Tsai, H. H., Tessier-Lavigne, M., and Miller, R. H. (2003) Netrin 1 mediates spinal cord oligodendrocyte precursor dispersal. *Development* **130,** 2095–2105
19. Jarjour, A. A., Manitt, C., Moore, S. W., Thompson, K. M., Yuh, S. J., and Kennedy, T. E. (2003) Netrin-1 is a chemorepellent for oligodendrocyte precursor cells in the embryonic spinal cord. *J. Neurosci.* **23,** 3735–3744
20. Su, Z., Cao, L., Zhu, Y., Liu, X., Huang, Z., Huang, A., and He, C. (2007) Nogo enhances the adhesion of olfactory ensheathing cells and inhibits their migration. *J. Cell Sci.* **120,** 1877–1887
21. Tong, X. P., Li, X. Y., Zhou, B., Shen, W., Zhang, Z. J., Xu, T. L., and Duan, S. (2009) Ca^{2+} signaling evoked by activation of Na^+ channels and Na^+/Ca^{2+} exchangers is required for GABA-induced NG2 cell migration. *J. Cell Biol.* **186,** 113–128
22. Liu, X., Wang, Y., Zhang, Y., Zhu, W., Xu, X., Niinobe, M., Yoshikawa, K., Lu, C., and He, C. (2009) Nogo-A inhibits necdin-accelerated neurite outgrowth by retaining necdin in the cytoplasm. *Mol. Cell. Neurosci.* **41,** 51–61
23. Kuo, E., Park, D. K., Tzvetanova, I. D., Leiton, C. V., Cho, B. S., and Colognato, H. (2010) Tyrosine phosphatases Shp1 and Shp2 have unique and opposing roles in oligodendrocyte development. *J. Neurochem.* **113,** 200–212
24. Ren, X. D., Kiosses, W. B., and Schwartz, M. A. (1999) Regulation of the small GTP-binding protein Rho by cell adhesion and the cytoskeleton. *EMBO J.* **18,** 578–585
25. Wu, J. Y., Feng, L., Park, H. T., Havlioglu, N., Wen, L., Tang, H., Bacon, K. B., Jiang, Zh., Zhang, Xc., and Rao, Y. (2001) The neuronal repellent Slit inhibits leukocyte chemotaxis induced by chemotactic factors. *Nature* **410,** 948–952
26. Wong, E. V., Kerner, J. A., and Jay, D. G. (2004) Convergent and divergent signaling mechanisms of growth cone collapse by ephrinA5 and slit2. *J. Neurobiol.* **59,** 66–81
27. Prasad, A., Qamri, Z., Wu, J., and Ganju, R. K. (2007) Slit-2/Robo-1 modulates the CXCL12/CXCR4-induced chemotaxis of T cells. *J. Leukocyte Biol.* **82,** 465–476
28. Uehata, M., Ishizaki, T., Satoh, H., Ono, T., Kawahara, T., Morishita, T., Tamakawa, H., Yamagami, K., Inui, J., Maekawa, M., and Narumiya, S. (1997) Calcium sensitization of smooth muscle mediated by a Rho-associated protein kinase in hypertension. *Nature* **389,** 990–994
29. Liang, X., Draghi, N. A., and Resh, M. D. (2004) Signaling from integrins to Fyn to Rho family GTPases regulates morphologic differentiation of oligodendrocytes. *J. Neurosci.* **24,** 7140–7149
30. Salter, M. W., and Kalia, L. V. (2004) Src kinases, a hub for NMDA receptor regulation. *Nat. Rev. Neurosci.* **5,** 317–328
31. Colognato, H., Ramachandrappa, S., Olsen, I. M., and ffrench-Constant, C. (2004) Integrins direct Src family kinases to regulate distinct phases of oligodendrocyte development. *J. Cell Biol.* **167,** 365–375
32. Levison, S. W., and Goldman, J. E. (1993) Both oligodendrocytes and astrocytes develop from progenitors in the subventricular zone of postnatal rat forebrain. *Neuron* **10,** 201–212
33. Chen, G., Sima, J., Jin, M., Wang, K. Y., Xue, X. J., Zheng, W., Ding, Y. Q., and Yuan, X. B. (2008) Semaphorin-3A guides radial migration of cortical neurons during development. *Nat. Neurosci.* **11,** 36–44
34. Ypsilanti, A. R., Zagar, Y., and Chédotal, A. (2010) Moving away from the midline. New developments for Slit and Robo. *Development* **137,** 1939–1952
35. Spassky, N., de Castro, F., Le Bras, B., Heydon, K., Quéraud-LeSaux, F., Bloch-Gallego, E., Chédotal, A., Zalc, B., and Thomas, J. L. (2002) Directional guidance of oligodendroglial migration by class 3 semaphorins and netrin-1. *J. Neurosci.* **22,** 5992–6004
36. Tsai, H. H., Macklin, W. B., and Miller, R. H. (2006) Netrin-1 is required for the normal development of spinal cord oligodendrocytes. *J. Neurosci.* **26,** 1913–1922
37. Ridley, A. J. (2001) Rho proteins, PI 3-kinases, and monocyte/macrophage

motility. *FEBS Lett.* **498,** 168–171
38. Hall, A. (1998) Rho GTPases and the actin cytoskeleton. *Science* **279,** 509–514
39. Etienne-Manneville, S., and Hall, A. (2002) Rho GTPases in cell biology. *Nature* **420,** 629–635
40. Cox, E. A., Sastry, S. K., and Huttenlocher, A. (2001) Integrin-mediated adhesion regulates cell polarity and membrane protrusion through the Rho family of GTPases. *Mol. Biol. Cell* **12,** 265–277
41. Stevenson, N. J., McFarlane, C., Ong, S. T., Nahlik, K., Kelvin, A., Addley, M. R., Long, A., Greaves, D. R., O'Farrelly, C., and Johnston, J. A. (2010) Suppressor of cytokine signaling (SOCS) 1 and 3 enhance cell adhesion and inhibit migration toward the chemokine eotaxin/CCL11. *FEBS Lett.* **584,** 4469–4474
42. Tabu, K., Ohba, Y., Suzuki, T., Makino, Y., Kimura, T., Ohnishi, A., Sakai, M., Watanabe, T., Tanaka, S., and Sawa, H. (2007) Oligodendrocyte lineage transcription factor 2 inhibits the motility of a human glial tumor cell line by activating RhoA. *Mol. Cancer Res.* **5,** 1099–1109
43. Narumiya, S., Ishizaki, T., and Uehata, M. (2000) Use and properties of ROCK-specific inhibitor Y-27632. *Methods Enzymol.* **325,** 273–284
44. Nobes, C. D., and Hall, A. (1999) Rho GTPases control polarity, protrusion, and adhesion during cell movement. *J. Cell Biol.* **144,** 1235–1244
45. Tsuji, T., Ishizaki, T., Okamoto, M., Higashida, C., Kimura, K., Furuyashiki, T., Arakawa, Y., Birge, R. B., Nakamoto, T., Hirai, H., and Narumiya, S. (2002) ROCK and mDia1 antagonize in Rho-dependent Rac activation in Swiss 3T3 fibroblasts. *J. Cell Biol.* **157,** 819–830
46. Wong, K., Ren, X. R., Huang, Y. Z., Xie, Y., Liu, G., Saito, H., Tang, H., Wen, L., Brady-Kalnay, S. M., Mei, L., Wu, J. Y., Xiong, W. C., and Rao, Y. (2001) Signal transduction in neuronal migration. Roles of GTPase activating proteins and the small GTPase Cdc42 in the Slit-Robo pathway. *Cell* **107,** 209–221
47. Rajasekharan, S., Bin, J. M., Antel, J. P., and Kennedy, T. E. (2010) A central role for RhoA during oligodendroglial maturation in the switch from netrin-1-mediated chemorepulsion to process elaboration. *J. Neurochem.* **113,** 1589–1597
48. Xu, H. T., Yuan, X. B., Guan, C. B., Duan, S., Wu, C. P., and Feng, L. (2004) Calcium signaling in chemorepellant Slit2-dependent regulation of neuronal migration. *Proc. Natl. Acad. Sci. U.S.A.* **101,** 4296–4301
49. Osterhout, D. J., Wolven, A., Wolf, R. M., Resh, M. D., and Chao, M. V. (1999) Morphological differentiation of oligodendrocytes requires activation of Fyn tyrosine kinase. *J. Cell Biol.* **145,** 1209–1218
50. Miyamoto, Y., Yamauchi, J., and Tanoue, A. (2008) Cdk5 phosphorylation of WAVE2 regulates oligodendrocyte precursor cell migration through nonreceptor tyrosine kinase Fyn. *J. Neurosci.* **28,** 8326–8337
51. Yeo, M. G., Oh, H. J., Cho, H. S., Chun, J. S., Marcantonio, E. E., and Song, W. K. (2011) Phosphorylation of Ser-21 in Fyn regulates its kinase activity, focal adhesion targeting, and is required for cell migration. *J. Cell. Physiol.* **226,** 236–247
52. Wolf, R. M., Wilkes, J. J., Chao, M. V., and Resh, M. D. (2001) Tyrosine phosphorylation of p190 RhoGAP by Fyn regulates oligodendrocyte differentiation. *J. Neurobiol.* **49,** 62–78
53. Brouns, M. R., Matheson, S. F., and Settleman, J. (2001) p190 RhoGAP is the principal Src substrate in brain and regulates axon outgrowth, guidance, and fasciculation. *Nat. Cell. Biol.* **3,** 361–367
54. Liu, G., Beggs, H., Jürgensen, C., Park, H. T., Tang, H., Gorski, J., Jones, K. R., Reichardt, L. F., Wu, J., and Rao, Y. (2004) Netrin requires focal adhesion kinase and Src family kinases for axon outgrowth and attraction. *Nat. Neurosci.* **7,** 1222–1232
55. Cohen, R. I., Rottkamp, D. M., Maric, D., Barker, J. L., and Hudson, L. D. (2003) A role for semaphorins and neuropilins in oligodendrocyte guidance. *J. Neurochem.* **85,** 1262–1278
56. Prestoz, L., Chatzopoulou, E., Lemkine, G., Spassky, N., Lebras, B., Kagawa, T., Ikenaka, K., Zalc, B., and Thomas, J. L. (2004) Control of axonophilic migration of oligodendrocyte precursor cells by Eph-ephrin interaction. *Neuron Glia Biol.* **1,** 73–83
57. Holmes, G. P., Negus, K., Burridge, L., Raman, S., Algar, E., Yamada, T., and Little, M. H. (1998) Distinct but overlapping expression patterns of two vertebrate slit homologs implies functional roles in CNS development and organogenesis. *Mech. Dev.* **79,** 57–72
58. Stein, E., and Tessier-Lavigne, M. (2001) Hierarchical organization of guidance receptors. Silencing of netrin attraction by slit through a Robo-DCC receptor complex. *Science* **291,** 1928–1938
59. Rajasekharan, S., Baker, K. A., Horn, K. E., Jarjour, A. A., Antel, J. P., and Kennedy, T. E. (2009) Netrin 1 and DCC regulate oligodendrocyte process branching and membrane extension via Fyn and RhoA. *Development* **136,** 415–426